SCEC Report
SCEC Project #22084

Experimental Investigation of Multi-Scale Flash Weakening

Frederick M. Chester
Judith S. Chester
Monica R. Barbery
Santa G. Bonnett

Department of Geology & Geophysics
Center for Tectonophysics
Texas A&M University

Research Category: **Integration and Theory**

Science Objectives: **P1d, P3c, P2d**

Duration: **1 February, 2021 to 31 January, 2023**

Introduction

The coefficient of friction is the macroscopic description of the shear resistance to sliding along an interface between solids that results from chemical and mechanical processes operating at microscopic-scale contacts (Bowden & Tabor, 1964; Dieterich, 1978; Rice, 2006; Beeler et al., 2008; Elbanna & Carlson, 2014; Aharonov & Scholz, 2018). Static and kinetic friction phenomena are well described by modern friction constitutive relations developed from microphysical contact models. In these models, the time dependence of static friction and the velocity dependence of kinetic friction arise from thermal-activated creep processes within the asperity volume and at the asperity contact junction. Two regimes of friction may be defined on the basis of the sliding velocity (V) relative to the critical weakening velocity (V_w), the quasi-static, rate- and state-friction regime where frictional heating rates are low and temperature at contact junctions is relatively constant, and the dynamic, flash-weakening regime where high work rates and localized sliding lead to flash heating of contact junctions and significant reductions in friction (Fig.1).

The flash-weakening relations that describe very-strong weakening behavior at seismic slip rates also have application to the nucleation and rupture propagation phase, and are appropriate for modeling dynamic rupture propagation, including crack-like or self-healing slip pulses, as well as understanding the low apparent strength of lithospheric faulting (e.g., Dunham et al., 2011a, b; Goldsby & Tullis, 2011; Noda et al., 2009; Sleep, 2019; Lambert & Lapusta, 2020). Although the magnitude of weakening documented in the laboratory is comparable to that often assumed in dynamic rupture models, the characteristic slip distance over which weakening occurs is different. Critical slip distances for weakening in laboratory tests are similar in magnitude to the assumed dimensions of microscopic contact junctions in microphysical contact models, that is on the order of tens of micrometers (e.g., Marone, 1998; Beeler et al., 2008). In contrast, the inferred slip distance for weakening during earthquake rupture is orders of magnitude larger, though admittedly not well constrained (e.g., Tinti et al., 2005; Rice et al., 2005). An important challenge is to reconcile the apparent difference in weakening distance between earthquakes and empirical friction relations derived from laboratory experiments. A key observation that may advance understanding is that natural faults are rough at all scales (e.g., Scholz & Aviles, 1986; Candela et al., 2012), unlike the sliding surfaces of rock samples prepared for laboratory friction experiments.

Elastic models of stress associated with slip along a surface with roughness characteristics similar to crustal faults illustrate the development of inhomogeneous stress that locally varies in magnitude between near-zero and the local yield strength of the solid media, and that surfaces are locally out of contact at the decimeter to mm length-scale depending on depth (e.g., Chester & Chester, 2000; Sagy & Lyakhovsky, 2019). During slip events, significant changes in local stress magnitude develop and progressively become more inhomogeneous over length-scales up to the magnitude of slip. At the first increment of slip, flash heating at microscopic asperity contacts produces nearly instantaneous weakening. With continued slip, however, the local surface temperature (T_S) increases, and additional weakening occurs through the dependence of V_w on T_S (Fig. 1). Our high-speed experiments on flat ground surfaces show that T_S is inhomogeneous at the mm scale, indicating that flash weakening is a multiscale process of thermal softening at micrometer-scale asperity contact surfaces and of inhomogeneous heating at the mm scale to increase T_S (Saber, 2017; Barbery et al., 2021). In addition, transient friction behaviors associated with flash-weakening may be characterized as a fading-memory transient behavior (e.g., Rice and Ruina, 1983) associated with flash heating and surface cooling at different contact-length and -time scales as slip progresses (e.g., Proctor et al., 2014).

We hypothesize that for sliding on self-affine, rough fault surfaces, the critical slip distance for friction by flash weakening will be proportional to earthquake slip, and thus cannot be defined directly in a typical laboratory experiment using samples that lack self-affine roughness over length

scales comparable to slip. Rather, the macroscopic dynamic-weakening friction-behavior should be determined by combination of appropriate experiments that inform modeling of transient friction up to the length scale of earthquake slip. Such a description of friction would be complementary to dynamic rupture modeling efforts that treat effects of fault roughness down to length scales just greater than the magnitude of earthquake slip (e.g., Dunham et al., 2011a, b).

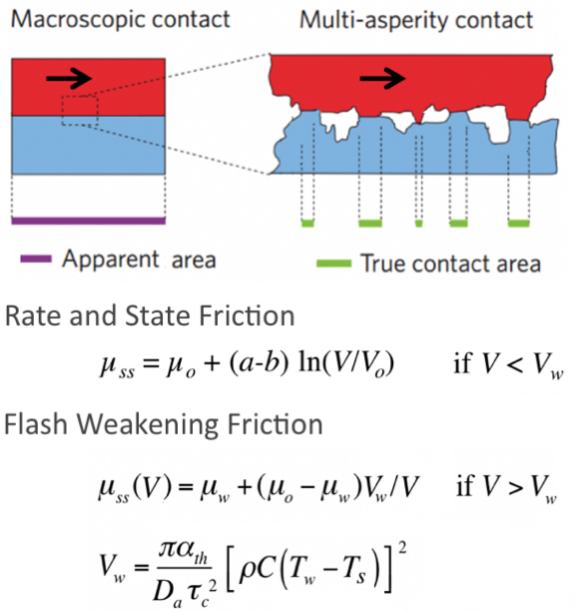

Fig. 1. The microphysical model of friction is based on the concept that microscopic scale roughness of surfaces form asperity contacts, and the fractional area of true contact is a function of the compressive (indentation) strength of the solid and the applied normal stress. The shear stress for sliding is the product of the shear strength of the contact junction interface and the true contact area. Thus, the coefficient of friction is simply the ratio of the shear strength of the asperity contact junctions to the compressive strength of the solid. The velocity dependence of rate-and-state friction, and flash-weakening friction, reflect thermal activated processes at contact junctions. Contact junction parameters D_a is junction size, τ_c is shear strength, T_w is the weakening temperature, and μ_w is the fully weakened friction. T_S is the local surface temperature, a and b are the direct and evolution parameters, respectively, and the other parameters are material properties.

The state of rough faults is characterized by inhomogeneity in local normal stress, slip magnitude, and slip history, all of which can vary with position. The basic question in the SCEC science plan addressing how the evolving structure, composition and physical properties of fault zones and surrounding rock affect shear resistance to seismic and aseismic slip has directed much of our experimental work reported here. Over our multi-year project, we experimentally investigated flash heating during high-speed frictional sliding in rock to better constrain and test the theoretical-based models of flash weakening (Rice, 2006; Beeler et al., 2008). Conventional theoretical models of flash heating at micrometer-scale contacts can explain dramatic reduction of friction at earthquake slip rates. The conventional model also treats the progressive rise in macroscopic surface temperature with displacement that further enhances reduction of friction (e.g., Proctor et al., 2014; Yao et al., 2016). We have conducted high-acceleration, high-speed friction experiments that mimic earthquake rupture and slip using a biaxial apparatus equipped with an IR camera to record flash temperature distributions on the sliding surfaces. Test blocks are machined to standardize surface patterns with two dominant length scales (μm and mm) of roughness that are consistent with roughness of natural faults (Brodsky et al., 2016; Candela et al., 2012).

Research Methods and Results

We tested friction on relatively large surfaces (totaling 75 cm^2) of rock blocks in double-direct shear (DDS) with our high-speed biaxial apparatus. The sliding surfaces are prepared by machining flat surfaces with a #60 grit precision grinding wheel to a root mean squared roughness of ~10^{-2} mm. We then grind a series of grooves in the surfaces to a depth of 50 μm, width of 3.175 or 1.588 mm, and spacing of 3.175 mm. The grooved pattern generates a series of flat-topped ridges, that correspond to

the original ground-flat surfaces. The ridges on the surfaces of opposing blocks are oriented 22.5° to the sliding direction, but in opposite sense (Fig. 2). The configuration allows us to dictate sliding histories of mm-scale contacts; more specifically it allows us to control the time (or magnitude of slip) that points on the ridge surfaces are in contact (Life Time, LT) and out of contact (Rest Time, RT). Both *LT=RT* and *LT>RT* (*LT*=2*RT*) geometries are tested. Using a high-speed IR camera, we image the moving block surface as it emerges during high-speed sliding to record the T_S distribution produced by flash heating (Fig.2).

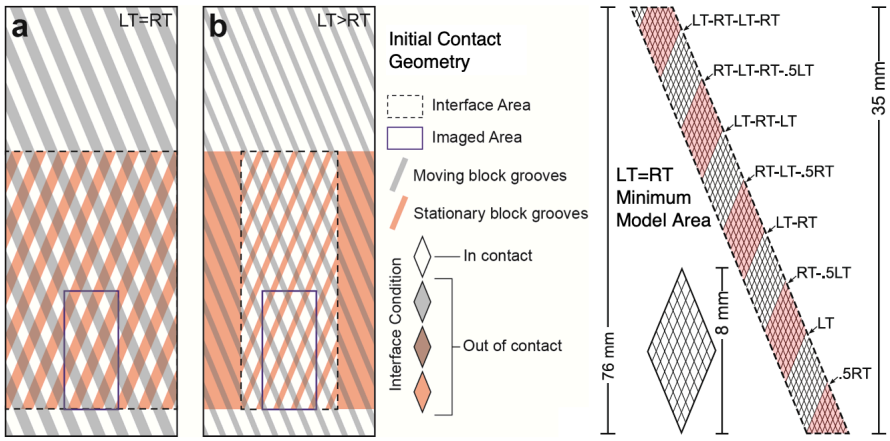

Fig. 2. Initial contact distributions for the two geometries examined: *LT=RT* and *LT>RT* (*LT*=2*RT*). Contact occurs only where ridges on the moving block juxtapose ridges on the stationary block. The macro-scopic contact area (a, b, dashed black lines) is reduced for *LT>RT* geometry to ensure the same mm-scale contact area for both geometries. The minimum model area for the LT=RT comprises 544 discrete 1mm^2 elements, with each element having a different phase and total number of cycles is shown on the right. The LT-RT cycle histories for selected elements are indicated to the right of the enlarged model area, with the first to last stage of the sequence labeled left-to-right. An analogous minimum model area for the LT>RT geometry is not shown here. The view of the interface is looking through the stationary block towards the moving block. Figure modified from Barbery et al., 2021.

We have conducted experiments on both *LT=RT* and *LT>RT* geometries employing velocity-steps from quasi-static to seismic sliding-rates (~0.1 to 1 m.s^{-1}) followed by sliding at constant velocity for up to 3.5 cm, but also with different magnitude decelerations to self-arrest. In addition, we have tested both conventional flat ground surfaces and *LT=RT* shaped surfaces at a range of normal stress from 2 to 20 MPa. We document that the T_S is inhomogeneous across the sliding surface, and overall the T_S increases with displacement as expected (Barbery et al., 2021). We document that the average T_S is greater and the friction is lower in the LT>RT tests compared to the LT=RT tests at similar velocity and normal stress. To determine the σ_L distribution at the mm-scale, we combine a one-dimensional thermal model with conventional flash-weakening relations that incorporates a T_S-dependence (Fig. 1) informed by the controlled mm-scale contact history (Barbery et al., 2021). Some contacts at early stages of slip experience σ_L exceeding 40 times the applied normal stress (σ_n), though most are in the range of 6-20 times. As sliding progresses, the σ_L at the hottest contacts decreases as contact area increases, leading to σ_L ranging from 2-6 times the applied σ_n on most contacts by 30 mm of slip. We find that increases in T_S that would decrease the coefficient of friction are buffered by wear processes that increase mm-scale contact area and gouge thickness and decrease the σ_L such that nearly constant friction is achieved in experiments at constant velocity (Barbery et al., 2021; Barbery et al., 2023). Notably, the distribution of σ_L with slip in *LT=RT* and *LT>RT* tests are consistent, and by analysis of many additional experiments conducted to date, the σ_L distribution with slip is now much better constrained (Fig. 3).

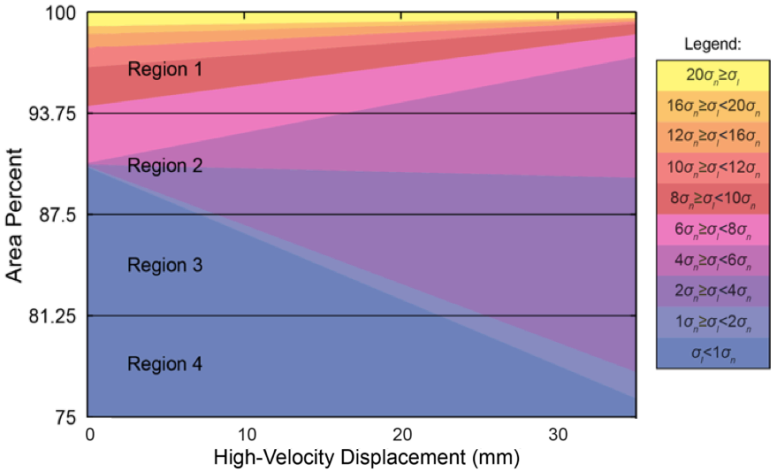

Fig. 3. Changes in the local normal stress, σ_L, distributions in area percent of the macroscopic surface with high-velocity displacement for all modeled ranges of σ_L. Each range is represented by a different color and labeled in the legend. For readability, the six highest ranges analyzed (i.e., > $20\sigma_n$) were combined into a single range. The σ_L distributions are averaged within four discretized regions separated by lines for our initial modeling of experiment results to determine constitutive parameters $\tau_c^2 D_a$, T_w, and μ_w for flash weakening in granite (*Fig. 1*). Figure from Barbery et al., 2023.

We use an iterative numerical simulation in a forward modeling approach to determine the values of the key parameters ($\tau_c^2 D_a$, T_w, and μ_w) of the flash weakening constitutive equations (Fig. 1). We model a subset of experiments that represent the range of behaviors (resulting from different controlled, independent parameters of sliding velocity, deceleration rate, LT and RT). The key inputs of the numerical simulation are the σ_L distribution (Fig. 3), the LT and RT for the appropriate minimum model area (Fig. 2), and the measured sliding velocity and normal stress history of each experiment. Systematic variation of the three constitutive parameters and comparing model outputs to experiment data (specifically, the friction versus displacement curves and T_S distributions) allow us to determine parameter values. In general, we find that in our high acceleration, high speed tests, the friction at relatively steady sliding rate are well described by the conventional flash-weakening model; however, observations of transient and hysteretic friction during the acceleration and deceleration phases of the sliding event are not as well described, and typically greater than observed.

We have investigated the hypothesis that the development of mm-scale hot contacts evident in thermographs of machined samples (with and without grooves) reflect local differences in stiffness and wear rates of the three main mineral phases of the granite (feldspar, quartz and biotite). Profilometry and mineral mapping show that the machine ground surfaces of our samples have a starting micrometer-scale roughness that is isotropic, homogeneous and independent of the mineralogy of the granite. In addition, comparing pre-sliding mineral maps with thermographs document a correlation between high-temperature spots and mineral type; specifically, we find that feldspar and quartz show greater probability and biotite the lowest probability of coinciding with hot spots, and the relative probability qualitatively correlates with elastic moduli for the three minerals. Observations also indicate that after several sequential friction tests, wear produces gouge layers up to >50 μm thick with a corrugated interfacial slip surface, whereas the worn rock surface bounding the gouge layer appears to display an isotropic, homogeneous roughness.

The conventional flash-weakening model considers only sliding motion between adhesive, micrometer-scale asperity contacts, such as occurs on ridges of our samples ground nominally flat. However, the development of mm-scale hot spots and wear product production and accumulation motivates a multi-scale flash-weakening model, where mm-scale shearing can occur in the accumulated wear product layer for durations several orders of magnitude greater than that of the micrometer-scale contacts. For this case we employ a thermal model with distributed heating over a half-width of 150 μm (Proctor et al., 2014; Barbery et al., 2023), which includes additional fitting parameters. Barbery et al. (2023) modeled eight of thirty-seven experiments that display the range of

behaviors in experiments with 4 different target velocities having constant or decreasing velocity profiles, and with both LT=RT and LT>RT. A representative example is shown in Fig. 4; however, see Barbery et al. (2023) for additional details and comparison of single scale and multi-scale, inhomogeneous local normal stress best-fits for individual tests, and comparison of non-global and global best-fits for individual tests. Overall, our multi-scale flash-weakening model incorporating inhomogeneous contact-scale normal stress resolves some outstanding transient and hysteretic friction observed in laboratory experiments, weakening is still not fully described and uncertainty regarding Westerly granite constitutive parameter values remains. Dynamic weakening models will be advanced by further incorporating wear processes and by considering processes acting over the mm-scale and above.

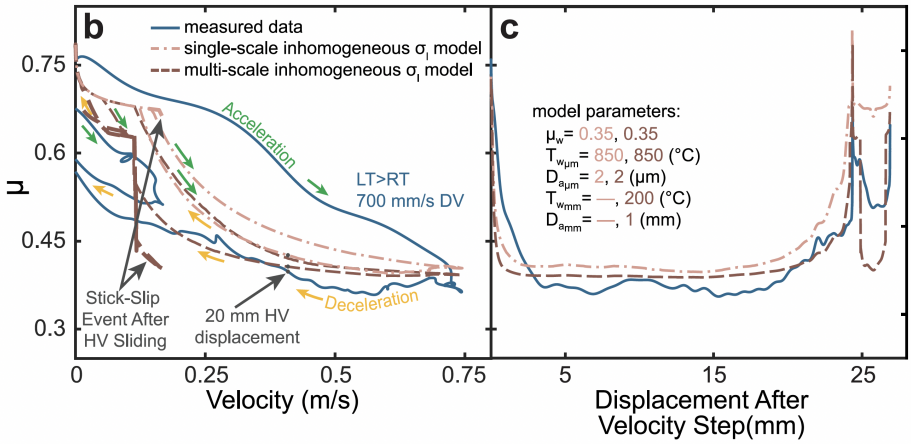

Fig. 4. Comparisons between modeled friction (dashed lines) and measured friction (solid lines) with sliding velocity (b) and displacement (c) for Experiment 436. Multi-scale model results for the non-global, best fitting parameter set (brown dashed line) are plotted alongside single-scale model results (pink dotted-dashed line). Acceleration and deceleration phases of slip are marked with green and yellow arrows, respectively. Figure from Barbery et al., 2023.

Conclusions

- Flash weakening in friction is likely an important process in earthquake rupture nucleation and seismic slip, and can be studied in our unique high speed and high acceleration biaxial apparatus
- High speed IR imaging demonstrates that flash surface-temperature at the millimeter and larger scale are inhomogeneous on rock interfaces during seismic slip
- Through use of standardized machined rock surfaces with multi-scale (μm and mm) roughness we can determine accurately the local normal stress distribution on sliding surfaces.
- Millimeter-scale contacts comprise ~10% of the apparent area, flash to 200˚C–400˚C, and support local normal stress 6–20 times the macroscopic normal stress
- Dynamic friction remains constant with increasing flash temperatures because wear increases contact area with slip and reduces local normal stress
- Incorporating mm-scale contact evolution along with weakening at both the μm- and mm-scale improves the flash-weakening model
- Flash weakening relations can describe observed friction throughout slip events but tend to underestimate and overestimate frictional strength during the accelerating and decelerating stages of high-speed sliding event.
- We suggest flash weakening models may be advanced by considering additional processes of fracture, wear, plowing and localization/delocalization processes at multiple length scales.

References

Aharonov, E., & Scholz, C. H. (2018). A physics-based rock friction constitutive law: Steady state friction. Journal of Geophysical Research: Solid Earth, 123, 1591–1614. https://doi.org/10.1002/2016JB013829

Barbery, M. R., F. M. Chester, J. S. Chester (2021), Characterizing the distribution of temperature and normal stress on flash heated granite surfaces at seismic slip rates. Journal of Geophysical Research: Solid Earth, 126, e2020JB021353, doi:10.1029/2020JB021353.

Barbery, M. R., F. M. Chester, J. S. Chester (2023), Investigating Dynamic Weakening in Laboratory Faults Using Multi-Scale Flash Heating Coupled With mm-Scale Contact Evolution. Journal of Geophysical Research: Solid Earth, 128, e2023JB027110.

Beeler, N. M., T. E. Tullis, and D. L. Goldsby (2008), Constitutive relationships and physical basis of fault strength due to flash heating, J. Geophys. Res., 113, B01401, doi:10.1029/2007JB004988.

Bowden, F. P., & Tabor, D. (1964). The friction and lubrication of solids (Vol. 2, No. 2). Oxford: Clarendon Press.

Brodsky, E. E., et al. (2016). Constraints from fault roughness on the scale-dependent strength of rocks. Geology 44(1): 19-22.

Candela, T., F. Renard, Y. Klinger, K. Mair, J. Schmittbuhl, and E. E. Brodsky (2012), Roughness of fault surfaces over nine decades of length scales, J. Geophys. Res., 117, B08409, doi:10.1029/2011JB009041.

Chester, F. M., and J. S. Chester (2000), Stress and deformation along wavy frictional faults, J. Geophys. Res., 105, 23,421-23,430.

Dieterich, J. H. (1978), Time-dependent friction and the mechanics of stick-slip, Pageoph., 116, 179-806.

Dunham, E. M., D. Belanger, L. Cong, and J. E. Kozdon (2011a). Earthquake ruptures with strongly rate-weakening friction and off-fault plasticity, Part 1: Planar faults, Bull. Seismol. Soc. Am., 101, 2296–2307.

Dunham, E. M., D. Belanger, L. Cong, and J. E. Kozdon (2011b), Earthquake Ruptures with Rate-Weakening Friction and Off-Fault Plasticity, Part 2: Nonplanar Faults, Bull. Seismol. Soc. Am., 101, 2308–2322, doi: 10.1785/0120100076.

Elbanna, A. E., and J. M. Carlson (2014), A two-scale model for sheared fault gouge: Competition between macroscopic disorder and local viscoplasticity, J. Geophys. Res. Solid Earth, 119, 4841–4859, doi:10.1002/2014JB011001.

Goldsby, D. L. and T. E. Tullis (2011). Flash Heating Leads to Low Frictional Strength of Crustal Rocks at Earthquake Slip Rates. Science 334(6053): 216-218.

Lambert, V. and N. Lapusta (2020), Rupture-dependent breakdown energy in fault models with thermo-hydro-mechanical processes, Solid Earth, 11(6), 2283-2302, doi: 10.5194/se-11-2283-2020

Marone, C. (1998), Laboratory-derived friction laws and their application to seismic faulting, Annu. Rev. Earth Planet. Sci., 26, 643-696.

Noda, H., E. M. Dunham, and J. R. Rice (2009), Earthquake ruptures with thermal weakening and the operation of major faults at low overall stress levels, J. Geophys. Res., 114, B07302, doi:10.1029/2008JB006143.

Proctor, B. P., et al. (2014). Dynamic weakening of serpentinite gouges and bare surfaces at seismic slip rates. Journal of Geophysical Research: Solid Earth 119: 8107-8131.

Rice, J. R. (2006). Heating and weakening of faults during earthquake slip. Journal of Geophysical Research 111(B5).

Rice, J.R., and A.L. Ruina (1983), Stability of steady frictional slipping, Journal of Applied Mechanics, 50, 343-349.

Rice, J. R., C. G. Sammis, and R. Parsons (2005). Off-fault secondary failure induced by a dynamic slip-pulse, Bull. Seismol. Soc. Am. 95, no. 1, 109–134, doi 10.1785/0120030166.

Saber, O. (2017), Development and characterization of a high-speed material-testing machine, and experimental analysis of frictional flash heating and dynamic weakening in rock, Ph.D. Dissertation, Texas A&M University, 161 p.

Sagy, A., & Lyakhovsky, V. (2019). Stress patterns and failure around rough interlocked fault surface. Journal of Geophysical Research: Solid Earth, 124, 7138–7154. https://doi-org.srv-proxy1.library.tamu.edu/10.1029/2018JB017006.

Scholz, C. H. and C. A. Aviles (1986). The fractal geometry of faults and faulting. Earthquake Source Mechanics. S. Das, J. Boatwright and C. H. Scholz. Washington, D.C., American Geophysical Union.

Sleep, N. H. (2019). Thermal weakening of asperity tips on fault planes at high sliding velocities. Geochemistry, Geophysics, Geosystems, 20, 1164–1188. https://doi.org/10.1029/2018GC008062.

Tinti, E., P. Spudich, and M. Cocco (2005), Earthquake fracture energy inferred from kinematic rupture models on extended faults, J. Geophys. Res., 110, B12303, doi:10.1029/2005JB003644.

Yao, L., S, Ma, J, D. Platt, A, R. Niemeijer, and T, Shimamoto (2016), The crucial role of temperature in high-velocity weakening of faults: Experiments on gouge using host blocks with different thermal conductivities, Geology, 44, 63–66, doi:10.1130/G37310.1